Synthesis, Characterization, and Crystal Structure of a (μ-Oxo)bis(μ-acetato)diiron(III) Complex with a Dinucleating Hexapyridine Ligand, 1,2-Bis[2-(bis(2-pyridyl)methyl)-6-pyridyl]ethane. The First Example of a Discrete (μ-Oxo)bis(μ-acetato)diiron(III) Complex with a Dinucleating Ligand

Masahito Kodera,*,† Hisashi Shimakoshi,† Masato Nishimura,‡ Hisashi Okawa,‡ Seiichiro Iijima,§ and Koji Kano†

Department of Molecular Science and Technology, Faculty of Engineering, Doshisha University, Tanabe, Kyoto 610-03, Japan, Department of Chemistry, Faculty of Science, Kyushu University, Hakozaki, Higashi-ku, Fukuoka 812, Japan, and National Institute of Bioscience and Human-Technology, Tsukuba, Ibaragi 305, Japan

Received January 31, 1996[⊗]

A mononucleating tripyridine ligand, 2-(bis(2-pyridyl)methyl)-6-methylpyridine (L^1), and a dinucleating hexapyridine ligand, 1,2-bis[2-(bis(2-pyridyl)methyl)-6-pyridyl]ethane (L^2), have been prepared. The reaction of a carbanion of 2,6-lutidine with 2-bromopyridine affords L^1 which is converted to L^2 quantitatively by treating with *tert*-butyllithium and 1,2-dibromoethane. (μ-Oxo)bis(μ-acetato)diiron(III) complexes $[Fe_2(O)(OAc)_2(L^1)_2](ClO_4)_2$ (**1**) and $[Fe_2(O)(OAc)_2L^2](ClO_4)_2$ (**2**) have been synthesized and characterized by means of infrared, UV/vis, mass, and Mössbauer spectroscopies and by measuring magnetic susceptibility and cyclic voltammograms. All the spectral data are consistent with the (μ-oxo)bis(μ-acetato)diiron(III) core structure in both **1** and **2**. A relatively strong molecular ion peak at *m/z* 865 corresponding to $[\{Fe_2O(OAc)_2L^2\}(ClO_4)]^+$ in a FAB mass spectrum of **2** suggests the stabilization of the (μ-oxo)bis(μ-acetato)diiron(III) core structure by L^2 in a solution state. The compound **2**·DMF·2-PrOH·H_2O, chemical formula $C_{44}Cl_2Fe_2H_{51}N_7O_{16}$, crystallizes in the monoclinic space group $C2/c$ with $a = 22.034(6)$ Å, $b = 12.595(5)$ Å, $c = 20.651(7)$ Å, $\beta = 121.49(2)°$, and $Z = 4$. The cation has 2-fold symmetry with the bridging oxygen atom on the 2-fold axis: Fe−(μ-O) = 1.782(5) Å, Fe−O−Fe = 123.6(6)°, and Fe···Fe = 3.142(3) Å. The diiron(III) core structure of **2** seems to be stabilized by encapsulation of the ligand. Compound **2** is the first example of a discrete (μ-oxo)bis(μ-acetato)diiron(III) complex with a dinucleating ligand.

Introduction

Oxo-bridged diiron moieties have been found as functional centers of biologically important non-heme iron proteins.[1,2] The oxo-bridged diiron structure has been found in the active sites of hemerythrin (Hr),[3] ribonucleotide reductase,[4] purple acid phosphatase,[5] and soluble methane monooxygenase (sMMO).[6] In Hr, the bridging oxygen atom acts as a proton acceptor to control the reversible dioxygen binding through a prototropy.[7] Recently, the structure of the hydroxylase component of sMMO has been revealed by X-ray analysis.[8] The sMMO has $\alpha_2\beta_2\gamma_2$ subunits, and each of the two α-subunits contains a diferric complex bridged by a hydroxide ion, a carboxylate ion of the side chain of glutamate of the enzyme, and an acetate ion which is incorporated accidentally from a buffer reagent.[8a] Although the active species of sMMO has not been clarified yet, it has been assumed to involve an oxo-bridged diiron(IV) moiety.[9] Functions of the (μ-oxo)diiron moiety of the other proteins have not been clarified yet.

Many oxo-bridged diiron complexes have been synthesized as model compounds of the diiron biosites.[10] The typical ligands for the diiron complexes are tripyrazolylborate[10f] and triazacyclononane derivatives.[10a] These ligands form spontaneously and afford corresponding (μ-oxo)bis(μ-acetato)diiron(III) complexes via self-organization of the two mononuclear iron(III) complexes in the presence of the carboxylate ion because of the thermodynamic stability of the resultant complexes. However, the core structures of these diiron complexes are kinetically unstable in a polar solvent. In order to obtain a more rigid (μ-oxo)bis(μ-

* To whom correspondence should be addressed.
† Doshisha University.
‡ Kyushu University.
§ National Institute of Bioscience and Human-Technology.
⊗ Abstract published in *Advance ACS Abstracts,* July 15, 1996.

(1) Lippard, S. J. *Angew. Chem., Int. Ed. Engl.* **1989**, *27*, 344.
(2) Kurtz, D. M., Jr *Chem. Rev.* **1990**, *90*, 585.
(3) (a) Wilkins, R. G.; Harrington, P. C. *Adv. Inorg. Biochem.* **1983**, *5*, 51−86. (b) Sheriff, S.; Hendrickson, W. A.; Smith, J. L. *J. Mol. Biol.* **1987**, *197*, 273. (c) Wilkins, P. C.; Wilkins, R. G. *Coord. Chem. Rev.* **1987**, *79*, 195.
(4) Sjoberg, B.-M.; Graslund, A. *Adv. Inorg. Biochem.* **1983**, *5*, 87.
(5) Antanaitis, B. C.; Aisen, P. *Adv. Inorg. Biochem.* **1983**, *5*, 111.
(6) (a) Dalton, H. In *Methane and Methanol Utilizers*; Murrell, J. C., Dalton, H., Eds.; Biotechnology Handbook 5; Plenum Press: New York, 1992; p 85. (b) Fox, B. G.; Lipscomb, J. D. *Methane Monooxygenase: A Novel Biological Catalyst for Hydrocarbon Oxidation*; Academic Press: New York, 1990; Vol. 1, p 367.
(7) (a) Shiemke, A. K.; Loehr, T. M.; Sanders-Loehr, J. *J. Am. Chem. Soc.* **1986**, *108*, 2437. (b) Solomon, E. I.; Zhang, Y. *Acc. Chem. Res.* **1992**, *25*, 343.
(8) Rosenzweig, A. C.; Frederick, C. A.; Lippard, S. J.; Nordlung, P. *Nature* **1993**, *366*, 537.
(9) (a) Feig, A. L.; Lippard, S. J. *Chem. Rev.* **1994**, *94*, 759. (b) Lipscomb, J. D. *Annu. Rev. Microbiol.* **1994**, *48*, 371.
(10) (a) Wieghardt, K.; Pohl, K.; Gebert, W. *Angew. Chem., Int. Ed. Engl.* **1983**, *22*, 727. (b) Chaudhuri, P.; Wieghardt, K.; Nuber, B.; Weiss, J. *Angew. Chem., Int. Ed. Engl.* **1985**, *24*, 778. (c) Wieghardt, K.; Pohl, K.; Ventur, D. *Angew. Chem., Int. Ed. Engl.* **1985**, *24*, 392. (d) Hartman, J.-A. R.; Rardin, R. L.; Chaudhuri, P.; Pohl, K.; Wieghardt, K.; Nuber, B.; Weiss, J.; Papaefthymiou, G. C.; Frankel, R. B.; Lippard, S. J. *J. Am. Chem. Soc.* **1987**, *109*, 7387. (e) Armstrong, W. H.; Lippard, S. J. *J. Am. Chem. Soc.* **1983**, *105*, 4837. (f) Armstrong, W. H.; Spool, A.; Papaefthymiou, G. C.; Frankel, R. B.; Lippard, S. J. *J. Am. Chem. Soc.* **1984**, *106*, 3653.
(11) Tanaka, N.; Kobayashi, Y.; Takamoto, S. *Chem. Lett.* **1977**, 107.

S0020-1669(96)00099-7 CCC: $12.00

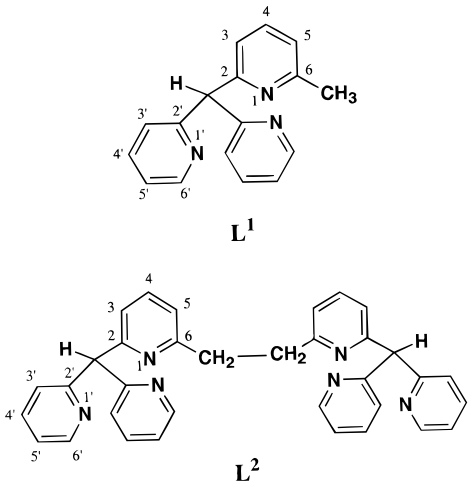

Figure 1. Chemical structure of L^1 and L^2.

carboxylato)diiron(III) complex, a few ligands which involve two tridentate coordination sites linked by an alkyl chain have already been prepared. For instance, Wieghardt et al.[12] reported that the (μ-oxo)bis(μ-acetato)diiron(III) core structure is stabilized when the 1,2-bis(1,4,7-triaza-1-cyclononyl)ethane ligand[11] (L^3) is used. Sessler et al.,[13] however, proposed the formation of a tetranuclear iron complex with a similar ligand system, 1,4-bis(1,4,7-triaza-1-cyclononyl)butane (L^4). The high nuclearity of the iron complex of L^4 has been demonstrated by the X-ray structure of the complex.[13] Before Sessler's work, Toftlund et al.[14] reported the synthesis and the crystal structure of a similar tetranuclear iron complex of tetrakis(2-pyridylmethyl)-1,4-butanediamine (L^5) and they also suggested that the iron complex reported by Wieghardt et al.[12] might better be formulated as a tetranuclear species. Although the dinucleating ligands such as L^3, L^4, and L^5 have been used to stabilize the (μ-oxo)bis(μ-acetato)diiron(III) core structure, no evidence has been obtained for the formation of the discrete (μ-oxo)bis(μ-carboxylato)diiron complex of the dinucleating ligand.

In order to obtain a thermodynamically and kinetically stable (μ-oxo)bis(μ-acetato)diiron(III) complex, a new dinucleating ligand, 1,2-bis[2-(bis(2-pyridyl)methyl)-6-pyridyl]ethane (L^2), has been prepared via a carbon-carbon homo-coupling of a carbanion of 2-(bis(2-pyridyl)methyl)-6-methylpyridine (L^1). The chemical structures of L^1 and L^2 are shown in Figure 1. This paper deals with the syntheses of the ligands L^1 and L^2 and their (μ-oxo)bis(μ-acetato)diiron(III) complexes, $[Fe_2(O)(OAc)_2(L^1)_2](ClO_4)_2$ (**1**) and $[Fe_2(O)(OAc)_2L^2](ClO_4)_2$ (**2**), and the characterization of these diiron(III) complexes. The structure of **2**·DMF·2-PrOH·H_2O has been determined by means of X-ray crystallography. Compound **2** is the first example of a discrete (μ-oxo)bis(μ-acetato)diiron(III) complex of a dinucleating ligand.

Experimental Section

Physical Measurements. Elemental analyses were performed at the Service Center of Elemental Analysis of Kyushu University. The analysis of iron content in the present iron complexes was carried out on a Shimadzu AA-680 atomic absorption/flame emission spectrophotometer. ^{1}H and ^{13}C NMR spectra (in $CDCl_3$) were recorded on a JEOL JNM-A 400 spectrometer using Me_4Si as an internal standard. The high resolution mass of L^2 was obtained on a JEOL JMS-AX505HA spectrometer in the Application Research Center of JEOL Ltd. Fast atom bombardment (FAB) mass spectra were obtained on a JEOL JMS-DX 300 spectrometer. Infrared (IR) spectra were taken on a JASCO IR-810 spectrometer on KBr disks or Nujol mulls. UV/vis absorption spectra were measured on a Shimadzu MPS-2000 multipurpose spectrophotometer at room temperature. Magnetic susceptibilities were measured in the range 80−300 K on a Faraday balance. The apparatus was calibrated with $[Ni(en)_3][S_2O_3]$.[15] The data of the diamagnetism of the constituent atoms were corrected by the use of Pascal's constants.[16] Cyclic voltammograms (CV) were recorded on an apparatus comprised of a Hokuto Denki HA-501 potentiostat and an HB-104 function generator. The CV measurements were carried out in acetonitrile or DMF (*ca.* 1×10^{-3} mol dm^{-3}) using $(Bu_4N)ClO_4$ as a supporting electrolyte. A three-electrode cell with a glassy-carbon working electrode, a platinum-coil auxiliary electrode and a saturated calomel reference electrode (SCE) was used. Mössbauer spectra were measured in the National Institute of Bioscience and Human-Technology at Tsukuba, Japan. The radio active source was ^{57}Co(Rh). The isomer shifts were reported relative to metallic iron foil.

Synthesis. 2-(Bis(2-pyridyl)methyl)-6-methylpyridine (L^1). In 200 mL of dry THF, 21.45 g (0.2 mol) of 2,6-lutidine was dissolved and the solution was cooled to −78 °C using a cooling bath under Ar. To the solution was added 250 mL of *n*-BuLi (1.66 M) in hexane at −78 °C under Ar. The cooling bath was removed and the mixture was stirred at room temperature for 24 h under Ar. To the resultant reddish brown solution was added 50 mL of *n*-BuLi (1.66 M) in hexane at −78 °C under Ar. The mixture was warmed to room temperature and stirred for 3 h. Then the solution was cooled to −78 °C and added to a solution of 70 g of anhydrous $ZnCl_2$ (0.51 mol) in 200 mL of dry THF. The mixture turned pale yellow. To the mixture were added 500 mg of $[Pd(PPh_3)_4]$ and 78 g (0.50 mol) of 2-bromopyridine with stirring, and it was heated to reflux. The mixture gradually turned red. Heating and stirring were continued for 20 h. Sticky red solids deposited. After the mixture was cooled to room temperature, the supernatant was removed by decantation. To the red solid was added 100 mL of an aqueous solution of 20.4 g of NaOH (0.51 mol) and 100 mL of an aqueous solution of 122.5 g of $Na_2S·9H_2O$ (0.51 mol), and the mixture was stirred for 1 h. The white precipitates generated were removed by filtration and washed with 200 mL of $CHCl_3$. The filtrate and the $CHCl_3$ washings were combined, and the organic layer was separated using a separation funnel. The aqueous layer was further extracted by $CHCl_3$ (2×100 mL). After drying over anhydrous Na_2SO_4, the $CHCl_3$ extracts were concentrated to dryness. Volatile byproducts were separated by vacuum distillation. The first distillate was a mixture of 2-bromopyridine and 2-*n*-butylpyridine. The second distillate was 2-methyl-6-(2-pyridylmethyl)pyridine (14 g, 0.076 mol, 38% yield). The brown residue was dissolved in 20 mL of chloroform and purified by silica gel column chromatography with chloroform/ethylacetate (2:1, v/v) as a developing solvent to give L^1 (12.5 g, 0.048 mol, 24% yield) as a pale yellow solid. L^1 was further purified by recrystallization from *n*-hexane. Anal. Calcd for $C_{17}H_{15}N_3$: C, 78.13; H, 5.78; N, 16.08. Found: C, 77.09; H, 5.78; N, 15.44. IR data [ν/cm^{-1}] on KBr disks: 3050, 3000, 2930, 1585, 1570, 1460, 1455, 1430, 1140, 1100, 1050, 1000, 790, 760, 750, 680, 645, 630, and 620. ^{1}H NMR data: (δ/ppm vs Me_4Si) in $CDCl_3$: 8.58 (d−q, 2H, py′-6), 7.62 (t−d, 2H, py′-4), 7.53 (t, 1H, py-4), 7.30 (d, 2H, py′-3), 7.18−7.12 (m, 3H, py-3, py′-5), 7.02 (d, 1H, py-5), 6.00(s, 1H, methine), and 2.53 (s, 3H, CH_3). ^{13}C NMR data: (δ/ppm vs Me_4Si) in $CDCl_3$: 161.32, 160.13, 157.94 (py-2, py-6, py′-2), 149.44 (py′-6), 136.74, 136.47, 124.16, 121.63, 121.43, 121.22 (py-3, py-4, py-5, py′-3, py′-4, py′-5), 63.99 (methine), and 24.52 (CH_3). Mass data: *m/z* 261 (M^+), 183 ($M - C_5H_4N$), 106 ($M - C_5H_4N - C_5H_3N$).

1,2-Bis[2-(bis(2-pyridyl)methyl)-6-pyridyl]ethane (L^2). In 200 mL of dry THF, 1.0 g of L^1 (3.8 mmol) was dissolved, and the solution was cooled to −78 °C under Ar. To the solution was added 10 mL of 1.7 M *tert*-BuLi in pentane. At that time the mixture turned red. The cooling bath was removed and the red solution was stirred at 0 °C under Ar for 4 h. To the solution was added 2.4 g of 1,2-dibromoethane (12.7 mmol). The mixture was stirred at room temperature for 12 h. The reaction was followed by TLC (AcOEt:$CHCl_3$ = 1:1). After 20

(12) Wieghardt, K.; Tolksdorft, I.; Herrmann, W. *Inorg. Chem.* **1985**, *24*, 1230.
(13) Sessler, J. L.; Sibert, J. W.; Lynch, V. *Inorg. Chem.* **1990**, *29*, 4143.
(14) Toftlund, H.; Murray, K. S.; Zwack, P. R.; Taylor, L. F.; Anderson, O. P. *J. Chem. Soc., Chem. Commun.* **1986**, 191.
(15) Curtis, N. F. *J. Chem. Soc.* **1961**, 3147.
(16) Mulay, L. N. *Theory and Applications of Molecular Paramagnetism*; Wiley: New York, 1976; p 491.

mL of H_2O was added to the reaction mixture, THF was removed on the rotary evaporator. The resultant mixture was extracted by CH_2Cl_2 (3 × 50 mL). After being dried over anhydrous Na_2SO_4, the extracts were concentrated to dryness using a rotary evaporator. The solid residue was spectroscopically pure. Further purification was done by recrystallization from $CH_2Cl_2-Et_2O$. Yield: 1.0 g (95%). Anal. Calcd for $C_{34}H_{28}N_6 \cdot H_2O \cdot 0.25(C_2H_5)_2O$: C, 75.50; H, 5.88; N, 15.09. Found: C, 75.07; H, 5.42; N, 14.67. The high resolution mass spectrum of L^2 was measured to analyze the elements. (calcd for $C_{34}H_{28}N_6$, *m/z* 520.2371 (M^+); found, *m/z* 520.2375 (M^+, 100%)). IR data [ν/cm^{-1}] on KBr disks: 3050, 3000, 2950, 2900, 2850, 1580, 1560, 1460, 1450, 1425, 1000, 800, and 750. ^{1}H NMR data: (δ/ppm vs Me_4Si) in $CDCl_3$: 8.55 (d−q, 4H, py′-6), 7.58 (t−d, 4H, py′-4), 7.42 (t, 2H, py-4), 7.26 (d, 4H, py′-3), 7.18−7.12 (m, 6H, py-3, py′-5), 6.83 (d-d, 2H, py-5), 5.96 (s, 2H, methine), and 3.14 (s, 4H, CH_2CH_2). ^{13}C NMR data: (δ/ppm vs Me_4Si) in $CDCl_3$: 161.46, 160.79, 159.95 (py-2, py-6, py′-2), 149.25 (py′-6), 136.42, 136.27, 124.06, 121.48, 121.25, 121.02 (py-3, py-4, py-5, py′-3, py′-4, py′-5), 64.13 (methine), and 37.16 (CH_2-CH_2). Mass data: *m/z* 520 (M^+), 442 ($M - C_5H_4N$), 351 ($M - C_5H_4N - C_5H_3N - CH_2$), 260 ($M - C_5H_4N - 2C_5H_3N - 2CH_2$), 183 ($M - C_5H_4N - 3C_5H_3N - 2CH_2$), 169 ($M - C_5H_4N - 3C_5H_3N - 3CH_2$).

Preparation of Metal Complexes. $[Fe_2O(OAc)_2(L^1)_2](ClO_4)_2 \cdot 0.5MeCN$ (1). In 3 mL of EtOH, 522 mg (2.0 mmol) of L^1 was dissolved (solution A). In 12 mL of H_2O, 924 mg (2.0 mmol) of $Fe(ClO_4)_3 \cdot 6H_2O$ and 410 mg (5.0 mmol) of AcONa were dissolved (solution B). Solution B was added dropwise to solution A with stirring at room temperature. The mixture turned dark brown. The mixture was stirred at room temperature for 4 h to give a greenish brown powder and allowed to stand for 12 h in a refrigerator. The powder was collected by suction filtration, washed by a small amount of EtOH, and dried *in vacuo*. The dried powder was dissolved in MeCN solution saturated with AcONa, and the resultant solution was diffused with Et_2O to give greenish brown crystals and a small amount of red crystals. AcONa was essential to obtain the greenish brown crystals. The red crystals were generated during the recrystallization as a minor product. It has been reported that red crystals of a bis(ligand)iron complex of tripyrazolylborate, $[Fe(HB(pz)_3)_2]^+$, are formed as a byproduct in the preparation of $[Fe_2O(OAc)_2(HB(pz)_3)_2]$ (**3**).[10f] The red crystals obtained in this study may be a bis(ligand)iron complex, $[Fe(L^1)_2](ClO_4)_3$, although it has not been characterized yet. Yield of **1**: 40%. Anal. Calcd for $C_{38}Cl_2Fe_2H_{36}N_6O_{13} \cdot 0.5CH_3CN$: C, 47.42; H, 3.83; N, 9.22; Fe, 11.31. Found: C, 47.90; H, 4.01; N, 9.14; Fe, 11.47. Molar conductance (Λ_M/S cm^2 mol^{-1}) in DMF: 250. UV/vis data [λ_{max}/nm (ϵ/dm^3 mol^{-1} cm^{-1})] in MeCN: 363 (6100), 445 (2000), 500 (830), and 678 (160). Selected IR data [ν/cm^{-1}] on KBr disks: 3070, 2930, 2810, 1600, 1568, 1540, 1478, 1440, 1350, 1140, 1105, 1085, 1020, 800, 760, 720, 660, 620, and 510.

$[Fe_2O(OAc)_2L^2](ClO_4)_2 \cdot DMF \cdot 2\text{-}PrOH \cdot H_2O$ ($2 \cdot DMF \cdot 2\text{-}PrOH \cdot H_2O$). In 5 mL of MeOH, 462 mg (1.0 mmol) of $Fe(ClO_4)_3 \cdot 6H_2O$ and 205 mg (2.5 mmol) of AcONa were dissolved and a dark brown solution was obtained. To this solution was added immediately 260 mg (0.5 mmol) of L^2 in 10 mL of MeOH. The solution turned reddish brown. The mixture was stirred at room temperature to give reddish brown microcrystals. After 30 min, the crystals were collected by suction filtration, washed by a small amount of MeOH, and dried *in vacuo*. The crystals were dissolved in DMF and 2-PrOH was placed on the solution carefully to prevent a quick mixing. Greenish brown crystals were generated by slow diffusion of 2-PrOH. Yield: 80% Anal. Calcd for $C_{44}Cl_2Fe_2H_{51}N_7O_{16}$: C, 47.33; H, 4.60; N, 8.78; Fe, 10.00. Found: C, 47.25; H, 4.45; N, 8.66; Fe, 10.23. Molar conductance (Λ_M/S cm^2 mol^{-1}) in DMF: 130. UV/vis data [λ_{max}/nm (ϵ/dm^3 mol^{-1} cm^{-1})] in MeCN: 340 (4900), 380 (4100), 478 (780), 507 (710), and 715 (120). Selected IR data [ν/cm^{-1}] on KBr disks: 3070, 3020, 2930, 2810, 1600, 1570, 1540, 1440, 1350, 1140, 1085, 1020, 760, 745, 660, 620, 585, and 530. FAB mass spectrum: *m/z* 865, $[\{Fe_2O(OAc)_2L^2\}(ClO_4)]^+$; 806, $[\{Fe_2O(OAc)L^2\}(ClO_4)]^+$; 766, $[\{Fe_2O(OAc)_2L^2\}]^+$; 646, $[Fe_2OL^2]^+$.

X-ray Structure Analysis of $2 \cdot DMF \cdot 2\text{-}PrOH \cdot H_2O$. Crystals suitable for the X-ray analysis were obtained from recrystallization by a slow diffusion of 2-PrOH into the solution of **2** in DMF. A crystal with approximate dimensions of 0.40 × 0.30 × 0.25 mm sealed in a glass capillary was used for the X-ray diffraction study. The intensities and the lattice parameters were obtained on a Rigaku AFC7R automated four-cycle diffractometer with graphite-monochromated Mo Kα radiation (λ = 0.710 69 Å) at 20 °C. The unit cell dimensions and the oriented matrix for data collection were obtained from a least-squares refinement using the setting angles of 25 carefully centered reflections in the range 25.18° < 2θ < 26.96°. The pertinent crystallographic parameters are summarized in Table 1. The intensity data were collected at a temperature of 20 ± 1 °C using the $\omega-2\theta$ scan technique to a maximum 2θ value of 50.0°. The collected octants were (h, k, $\pm l$). Of the 4688 reflections which were collected, 4507 were unique (R_{int} = 0.135). Three standard reflections were monitored before every 150 measurements and showed no systematic decrease in intensity. An empirical absorption correction based on azimuthal scans of several reflections was applied which resulted in transmission factors ranging from 0.88 to 1.00.[25] The data were corrected for Lorentz and polarization effects. Corrections for extinction effects were not made.

Table 1. Crystal Data for $[Fe_2(O)(OAc)_2(hexpy)](ClO_4)_2 \cdot DMF \cdot 2\text{-}PrOH \cdot H_2O$

chem formula	$C_{44}Cl_2Fe_2H_{51}N_7O_{16}$
fw	1116.53
cryst syst	monoclinic
space group	*C*2/c
a/Å	22.034(6)
b/Å	12.595(5)
c/Å	20.651(7)
β/deg	121.49(2)
V/Å^3	4886(2)
Z	4
T/°C	20
D_c/g cm^{-3}	1.493
D_m/g cm^{-3}	1.50
radiation, Å	Mo Kα (λ = 0.710 73)
μ/cm^{-1}	7.76
R^a	0.083
R_w^b	0.089
GOF index	2.43

[a] $R = \sum||F_o| - |F_c||/\sum|F_o|$. [b] $R_w = [\sum w(|F_o| - |F_c|)^2/\sum w(F_o)^2]^{1/2}$, where $w = 1/\sigma^2(F_o)$.

The structure of **2** was solved by the direct method and expanded using Fourier techniques. The solvent molecules, the perchlorate anion, and the bridging ethylenic carbon atoms in the ligand are disordered. The nonhydrogen atoms except for the disordered atoms were refined anisotropically, while the rest were refined isotopically. The oxygen atom of the μ-oxo bridge and some atoms of the solvent molecules were found to lie on the 2-fold axis and each atom was assigned an occupancy factor of 0.5 in the least-squares refinement. The disordered ethylenic carbon atoms were also assigned occupancy factors of 0.5 in the least-squares refinement. The final cycle of full-matrix least-squares refinement was based on 1978 observed reflections ($I > 3.00\sigma(I)$). The disorder models of the solvent molecules and the perchlorate anion were not determined correctly. A water molecule, which was predicted to exist in the crystal by the elemental analysis, was not found from the difference-Fourier map. These facts may be the reason the final *R*

(17) (a) Kumada, M. *Pure Appl. Chem.* **1980**, *52*, 669. (b) Negishi, E. *Acc. Chem. Res.* **1982**, *15*, 340.
(18) Bishop, J. J.; Davison, A.; Katcher, M. L.; Lichtenberg, D. W.; Merrill, R. E.; Smart, J. C. *J. Organomet. Chem.* **1971**, *27*, 241.
(19) Hayashi, T.; Konishi, M.; Kobori, Y.; Kumada, M.; Higuchi, T.; Hirotsu, K. *J. Am. Chem. Soc.* **1984**, *106*, 158.
(20) Kauffmann, T.; Beissner, G.; Sahm, W.; Woltermann, A. *Angew. Chem., Inte. Ed. Engl.* **1970**, *9*, 808.
(21) Geary, W. J. *Coord. Chem. Rev.* **1971**, *7*, 81.
(22) Garbett, K.; Darnall, D. W.; Klotz, I. M.; Williams, R. J. P. *Arch. Biochem. Biophys.* **1969**, *135*, 419.
(23) Reem, R. C.; McCormick, J. M.; Richardson, D. E.; Delvin, F. J.; Stephens, P. J.; Musselman, P. L.; Solomon, E. I. *J. Am. Chem. Soc.* **1989**, *111*, 4688.
(24) A preliminary data for X-ray crystal structure analysis of **1** also supports the discrete dinuclear core structure. However, the reliability factors are not high enough to be reported.
(25) North, A. C. T.; Phillips, D. C.; Mathews, F. S. *Acta Crystallogr., Sect. A* **1968**, *A24*, 351

Table 2. Final Atomic Coordinations with Estimated Standard Deviations in Parentheses of 2·DMF·2-PrOH·H_2O

atom	x	y	z	B_{eq}[a]/Å^2
Fe	0.47033(8)	0.8239(10)	0.16234(9)	3.35(3)
Cl	0.2024(3)	0.1462(5)	0.7362(3)	9.3(1)
O(1)	0.5000	0.7570(8)	0.2500	4.7(3)
O(2)	0.4029(4)	0.9267(6)	0.1707(4)	4.1(2)
O(3)	0.5502(4)	0.9354(6)	0.2041(4)	4.2(2)
O(4)	0.133(1)	0.138(2)	0.675(1)	19.1(7)
O(5)	0.217(2)	0.236(3)	0.769(2)	29(1)
O(6)	0.248(1)	0.138(2)	0.711(1)	25(1)
O(7)	0.218(1)	0.068(2)	0.788(1)	22.5(9)
O(8)	0.9811	−0.0843	0.1774	19.0368
O(9)	0.7231	0.2822	0.5480	17.0768
N(1)	0.3832(5)	0.7116(8)	0.0958(5)	4.4(2)
N(2)	0.5232(5)	0.7270(7)	0.1182(5)	3.8(2)
N(3)	0.4317(5)	0.9122(8)	0.0553(5)	3.9(2)
N(4)	0.8132	0.2143	0.5582	29.0540
C(1)	0.3453(7)	0.665(10)	0.1209(7)	6.7(4)
C(2)	0.2860(7)	0.606(10)	0.0758(8)	6.0(4)
C(3)	0.2628(7)	0.594(10)	0.0015(8)	5.7(4)
C(4)	0.3035(6)	0.637(10)	−0.0253(6)	5.1(3)
C(5)	0.3633(5)	0.6956(6)	0.0218(6)	3.8(3)
C(6)	0.4107(6)	0.7376(9)	−0.0047(6)	3.9(3)
C(7)	0.4867(6)	0.7011(9)	0.0438(6)	3.8(3)
C(8)	0.5167(6)	0.6414(9)	0.0119(7)	4.4(3)
C(9)	0.5862(7)	0.608(10)	0.0575(8)	5.7(3)
C(10)	0.6240(7)	0.637(10)	0.1323(8)	5.8(3)
C(11)	0.5923(6)	0.696(10)	0.1628(7)	5.1(3)
C(12)	0.4085(6)	0.8584(9)	−0.0092(6)	3.6(2)
C(13)	0.3855(6)	0.911(10)	−0.0782(6)	5.0(3)
C(14)	0.3868(7)	1.018(10)	−0.0122(8)	5.5(3)
C(15)	0.4113(7)	1.073(10)	−0.1319(6)	6.1(3)
C(16)	0.4330(6)	1.0181(10)	−0.0795(7)	5.4(3)
C(17)	0.387(10)	0.625(20)	0.210(10)	4.3(5)
C(17*)	0.630(10)	0.714(20)	0.251(10)	4.9(5)
C(18)	0.4074(6)	0.9627(9)	0.2297(6)	4.1(3)
C(19)	0.3562(8)	1.048(10)	0.2187(7)	6.7(4)
C(20)	1.0000	−0.1139	0.2500	26.1982
C(21)	1.0000	−0.1940	0.2500	28.3341
C(22)	0.9874	−0.2427	0.1790	21.6822
C(23)	0.7500	0.2500	0.5000	15.3467
C(24)	0.8621	0.1896	0.5649	29.5796
C(25)	0.7583	0.2213	0.5535	21.5696

[a] $B_{eq} = 8\pi^2/3(U_{11}(aa^*)^2 + U_{22}(bb^*)^2 + U_{33}(cc^*)^2 + 2U_{12}aa^*bb^*\cos\gamma + 2U_{13}aa^*cc^*\cos\beta + 2U_{23}bb^*cc^*\cos\alpha)$.

Scheme 1

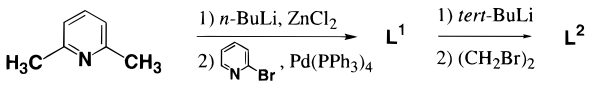

value could not be reduced below 0.083. The SHELXS-86[26] and teXsan[27] programs were used for solution and refinement of the structure, respectively. Atomic scattering factors were taken from the literature.[28] Additional material available from the Cambridge Crystallographic Data Center, comprises observed and calculated structure factors, H-atom coordinates, thermal parameters, and full bond distances and angles.

Results and Discussion

Preparation of Ligands L^1 and L^2. The synthetic route of the tripyridine ligand (L^1) and the dinucleating hexapyridine ligand (L^2) is shown in Scheme 1. Compound L^1 was prepared by the cross-coupling reaction[17] between the carbanion of 2,6-lutidine and 2-bromopyridine. We examined two synthetic pathways. One of them is a stepwise reaction via 2-methyl-6-(2-pyridylmethyl)pyridine as a synthetic intermediate. Another is a one-pot reaction involving a double cross-coupling reaction of the carbanion of 2,6-lutidine with 2-bromopyridine. The latter was superior to the former in the total yield of L^1. Two kinds of palladium complexes, $[Pd(PPh_3)_4]$ and $[PdCl_2(dppf)]$ (dppf = 1,1′-bis(diphenylphosphino)ferrocene),[18] were tested as a catalyst for the cross-coupling reaction. Although $[PdCl_2(dppf)]$ was a better catalyst for preparing 2-methyl-6-(2-pyridylmethyl)pyridine, it was inferior to $[Pd(PPh_3)_4]$ in obtaining L^1. Palladium(0) seems to be more appropriate to the double cross-coupling reaction in comparison to palladium(II). Since it is known that organozinc complexes provide good yields in cross-coupling reactions with organic halides compared with corresponding organolithiums,[19] zinc chloride was used to convert the lithiated 2,6-lutidine to the zinc complex in this study. The yield of L^1 was improved by the use of zinc chloride.

We modified a homocoupling reaction of lithiated methylpyridine derivatives, which was originally reported by Kauffmann et al,[20] to obtain L^2. An excess amount of *t*-BuLi was used to generate the dilithiated dianion of L^1. The oxidative coupling of the dianion using 1,2-dibromoethane as an oxidant afforded L^2 quantitatively. The ^{1}H NMR spectrum of L^2 is almost the same as that of L^1 because of the C_2 symmetric structure of L^2, except for the signals due to the protons of the ethylenic spacer, $-(CH_2)_2-$, and the 4-H and 5-H protons (see the numbering in Figure 1). A singlet peak of the ethylenic protons of L^2 appears at 3.14 ppm. The chemical shifts of 4-H and 5-H protons of the two pyridyl groups attached to the ethylenic spacer in L^2 appear at the higher magnetic fields relative to those of the corresponding H atoms in L^1 by 0.11 and 0.19 ppm, respectively. This may be due to a ring-current effect of the pyridyl groups, indicating that the two pyridyl groups weakly stack parallel to one another.

Preparation of Iron Complexes, 1 and 2. A dark brown solution of 5 equiv of AcONa and 2 equiv of $Fe(ClO_4)_3·6H_2O$ in MeOH turned reddish brown upon addtion of 1 equiv of L^2. Compound **2** was easily obtained almost quantitatively from the solution as microcrystals. Compound **2** is soluble in polar solvents such as MeCN and DMF. It should be noticed that **2** in MeCN or DMF does not show any spectral change on standing for several months at room temperature. The molar conductance of **2** in DMF is Λ_M 130 S cm^2 mol^{-1}, being in the range of those reported for 2:1 electrolytes (130−170 S cm^2 mol^{-1}).[21] The DMF solution of **2** was used to measure the FAB mass spectrum. The major peaks at *m/z* 865, 806, 766, and 646 are assigned to $[\{Fe_2O(OAc)_2L^2\}(ClO_4)]^+$, $[\{Fe_2O(OAc)L^2\}(ClO_4)]^+$, $[Fe_2O(OAc)_2L^2]^+$, and $[Fe_2OL^2]^+$, respectively. The fact that the (μ-oxo)bis(μ-acetato)diiron core structure is observed in the fragments indicates a high stability of the dinuclear core structure of **2**. Taking into account the fact that there has been no example of a discrete (μ-oxo)bis(μ-acetato)-diiron(III) complex with a dinucleating ligand, L^2 seems to have a specific structure for stabilizing the dinuclear core structure. This is demonstrated by the crystal structure of **2**·DMF·2-PrOH·H_2O (*vide infra*).

Since L^1 is a tridentate ligand having three π-nitrogen donors similar to tripyrazolylborate, $HB(pz)_3$,[10f] it is expected that the (μ-oxo)bis(μ-acetato)diiron(III) complex of L^1 **1** can be obtained by using a method similar to that for preparation of $[Fe_2O(OAc)_2(HB(pz)_3)_2]$, **3**. Addition of an aqueous solution of AcONa and the metal source to the ethanolic solution of L^1 affords crude **1** as a greenish brown powder. Crude **1** was purified by recrystallization. Two different colored crystals were obtained. The greenish brown crystals were mainly obtained on recrystallization in MeCN saturated with AcONa. The

(26) Sheldrick, G. M. *Acta Crystallogr., Sect A* **1990**, *46*, 467.
(27) Single crystal structure analysis software, version 1.6, Molecular Structure Corporation, the Woodlands, TX, 1993.
(28) *International Tables for X-ray Crystallography*; Kynoch Press: Birmingham, U.K., 1974; Vol. 4.

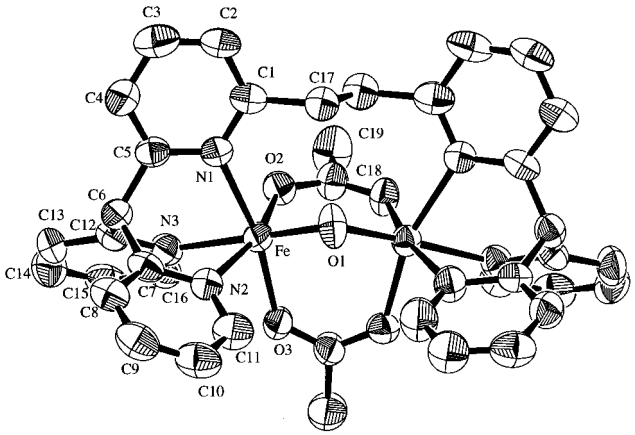

Figure 2. ORTEP view of the cation of **2** with the atom numbering scheme. The 50% probability thermal ellipsoids are shown. Hydrogen atoms and one of the disordered ethylenic spacers have been omitted.

Table 3. Selected Bond Distances (Å) and Angles (deg) for **2**

Bond Distances					
Fe···Fe	3.142(3)				
Fe−O(1)	1.782(5)	Fe−O(2)	2.045(8)	Fe−O(3)	2.056(7)
Fe−N(1)	2.196(9)	Fe−N(2)	2.188(9)	Fe−N(3)	2.209(9)
Bond Angles					
O(1)−Fe−O(2)	96.3(3)	O(1)−Fe−O(3)	96.7(3)		
O(1)−Fe−N(1)	93.9(3)	O(1)−Fe−N(2)	99.6(3)		
O(1)−Fe−N(3)	177.5(4)	O(2)−Fe−O(3)	91.9(3)		
O(2)−Fe−N(1)	91.4(3)	O(2)−Fe−N(2)	163.1(3)		
O(2)−Fe−N(3)	81.3(3)	O(3)−Fe−N(1)	168.4(3)		
O(3)−Fe−N(2)	91.7(3)	O(3)−Fe−N(3)	82.7(3)		
N(1)−Fe−N(2)	82.0(3)	N(1)−Fe−N(3)	86.8(3)		
N(2)−Fe−N(3)	82.8(3)	Fe−O(1)−Fe	123.6(6)		

greenish brown crystals are characterized to be the (μ-oxo)bis(μ-acetato)diiron(III) complex **1** as described below.

Crystal Structure of 2·DMF·2-PrOH·H_2O. The ORTEP view of the cation of **2**, $[Fe_2O(OAc)_2L^2]^{2+}$, is shown in Figure 2 together with the numbering scheme. The cation lies on a crystallographic 2-fold axis and, accordingly, has exact 2-fold symmetry. The bridging oxygen atom lies on the 2-fold axis. The iron atoms are each coordinated to one oxygen atom of the μ-oxo bridge, two oxygen atoms of the μ-acetato bridges and three nitrogen atoms of L^2 in an axially distorted octahedral geometry. The selected bond distances and bond angles are summarized in Table 3.

The ethylenic carbon atoms of L^2 were found to be disordered. The disordered carbon atom appears as a distinct peak on the difference-Fourier map. Reasonable temperature factors were obtained for the carbon atom, when a multiplicity of 0.5 was assigned. Therefore, equal amounts of two orientations of $[Fe_2O(OAc)_2L^2]^{2+}$ are related to one another by rotation about the crystallographic 2-fold axis. The rotation necessitates the movement of all the atoms of $[Fe_2O(OAc)_2L^2]^{2+}$ except for the oxygen atom on the 2-fold axis. However, the crystal structure analysis clearly indicates that the cationic part is rigid without any serious disorder except for the ethylenic carbon atoms. This suggests that the corresponding atoms in the two orientations are placed at an identical position except for the disordered ethylenic carbon atoms. Since the actual molecular structure does not have two ethylenic spacers, one of the disordered ethylenic spacers is deleted in the ORTEP diagram to prevent misunderstanding.

The X-ray structural study clearly demonstrates the discrete dinuclear structure of **2**. Ligand L^2 encapsulates the (μ-oxo)bis(μ-acetato)diiron(III) core. The NMR spectrum of L^2 suggests the partial stacking of two pyridine rings which are connected to each other by the ethylenic spacer. Such a preorganization of the ligand may be favorable for forming the discrete μ-oxo-di-μ-acetatodiiron(III) complex and can prevent the formation of a tetranuclear complex. The structural features of the diiron core of **2** are summarized in Table 4 together with comparable data for azido−metHr,[3b,22] two well characterized (μ-oxo)bis(μ-acetato)diiron(III) complexes of the general formula $[Fe_2O(OAc)_2L_2]^{2+}$ (L = $HB(pz)_3$ (**3**)[10f] and 1,4,7-trimethyl-1,4,7-triazacyclononane (**4**)[10d]) and two structurally determined tetranuclear complexes of dinucleating ligands $[Fe_2O(OAc)_2L]_2^{4+}$ (L = L^4 (**5**)[13] and L^5 (**6**)[14]). The bond lengths and the bond angles of the (μ-oxo)bis(μ-acetato)diiron(III) core of **2** are similar to those reported for compounds **3**−**6**. In particular, the distances Fe···Fe = 3.142(3) Å and Fe−O(1) = 1.782(5) Å and the Fe−O(1)-Fe angle = 123.6(6)° for **2** are almost the same as 3.146(1) Å, 1.788(2) Å, and 123.6(1)° for **3**, respectively, within the range of the standard deviations, indicating that the diiron(III) core structures of **2** and **3** are almost identical. This is probably due to the favorable preorganization of L^2 for the formation of the diiron(III) core and the similar aromatic nitrogen donor sets, three pyridines for each iron atom in L^2 and three pyrazoles in $HB(pz)_3$. The structural parameters of both **2** and **3** are more similar to the azido−metHr than those of the other model compounds as shown in Table 4. The structure of **2** should be more rigid than **3** since L^2 is the dinucleating ligand. A model compound of diiron biosites is required to simultaneously have structural similarity and high stability of the diiron core. In general, such requirements involving an antimony are not easily satisfied. However, **2** has remarkable features which satisfy these two requirements. Therefore, **2** may be one of the most promising model for the diiron biosites.

Physicochemical Properties of the Complexes. Two intense bands typical of bridging acetate groups are observed at $\nu_{asym}(CO_2)$ = 1540 cm^{-1} and $\nu_{sym}(CO_2)$ = 1440 cm^{-1} in the IR spectra of both **1** and **2**. The ν_{sym}(Fe−O−Fe) and ν_{asym}(Fe−O−Fe) bands at 530 and 745 cm^{-1}, respectively, for **2** are similar to those at 528 and 751 cm^{-1}, respectively, reported for **3**.[10f] The ν_{asym}(Fe−O−Fe) band for **2** is slightly lower than 770 cm^{-1} for the tetranuclear complex **6**.[14] The (Fe−O−Fe) vibration bands at 510 and 720 cm^{-1} for **1** appear at the lowest wave-numbers among related compounds. The other spectroscopic and magnetic data of **1**, **2**, **3**, **4**, **6**, and azido−metHr are summarized in Table 5. The UV/vis spectral features of both **1** and **2** are similar to those of the other model compounds and azido−metHr. The so-called oxo dimer region[23] (300−400 nm) of both **1** and **2** is not so clear, but it is similar to those of the other compounds. Two bands with medium intensities at 440−520 nm are commonly observed for these model compounds. These bands are assigned to ligand field transitions and a spin flip within the e_g orbitals.[2] The electronic absorption and IR spectral data indicate that both **1** and **2** have a similar (μ-oxo)bis(μ-acetato)diiron(III) core structure. Since L^1 is a simple tridentate ligand similar to $HB(pz)_3$, there is no reason *for* a higher nuclearity such as the tetranuclear species to stabilize **1**. Therefore, it may be concluded that **1** is also a discrete (μ-oxo)bis(μ-acetato)diiron(III) complex.[24]

The isomer shifts (δ) and the quadrupole splitting (ΔE_Q) values of **2** and its related compounds are also shown in Table 5. The ΔE_Q value of **2** is the largest among the model compounds shown here, and the δ value of **2** is in the range of those reported for related compounds including azido−metHr (0.47−0.52 mm s^{-1}). It has been reported that μ-oxo bridged diiron(III) complexes exhibit unusually large ΔE_Q values among high-spin ferric complexes due to the short Fe−O(μ-oxo) bond.[2]

Table 4. Structural Data for Complexes **2**−**6** and Azido−metHr

	dinuclear complexes			tetranuclear complexes		
	2	**3**	**4**	**5**	**6**	azido−metHr
Fe−O/Å	1.782(5)	1.788(2) 1.780(2)	1.800(3)	1.793(3) 1.761(6)	1.794(3)	1.79
Fe−N, cis to μ-oxo(av)/Å	2.196(9)	2.153(3)	2.198(4)	2.126(2)	2.136(11)	2.13
Fe−N, trans to μ-oxo (av)/Å	2.209(9)	2.188(3)	2.268(6)	2.268(3)	2.307(5)	2.24
Fe---Fe, within core/Å	3.142(3)	3.146(1)	3.12(4)	3.076(1)	3.129(2)	3.23
Fe−O−Fe/deg	123.6(6)	123.6(1)	119.7(1)	119.84(14)	121.3(3)	130

Table 5. Spectral and Magnetic Data for Complexes **1**−**4** and **6** and Azido−metHr

	dinuclear complexes				tetranuclear complex	
	1	**2**	**3**	**4**	**6**	azido−metHr
J/cm^{-1}	*b*	−95	−121	−119	−120	−134[a]
λ_{max}/nm	678 (80)	715 (60)	695 (70)	734 (60)	724 (123)	680 (95)
(ϵ/cm^{-1} mol^{-1} dm^3 of Fe)	500 (415)	507 (355)	492 (460)	519 (600)	499 (422)	446 (1850)
	445 (1000)	478 (390)	457 (505)	475 (780)	460 (521)	
	363 (3050)	380 (2050)	339 (4635)	345 (5250)	344 (5303)	380 sh (2150)
		340 (2950)				326 (3375)
δ/mm s^{-1} at 4.2 K	*b*	0.52	0.52	0.47	0.48	
δ/mm s^{-1} at 77 K	*b*	0.51		0.47		0.50
ΔE_Q/mm s^{-1} at 4.2 K	*b*	1.79	1.60	1.50	1.39	
ΔE_Q/mm s^{-1} at 77 K	*b*	1.79		1.50		1.91
references	this work	this work	10f	10d	14	10f

[a] J value of metHr. [b] Not determined.

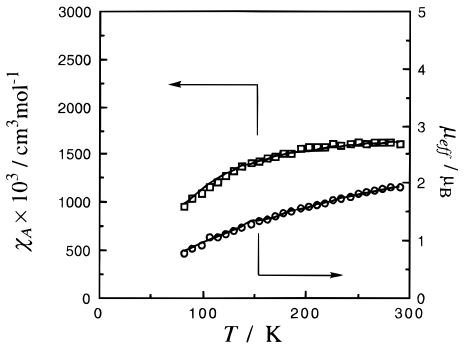

Figure 3. Temperature dependence of atomic magnetic susceptibility, χ_A (□), and magnetic moment, μ_{eff} (○), of **2**.

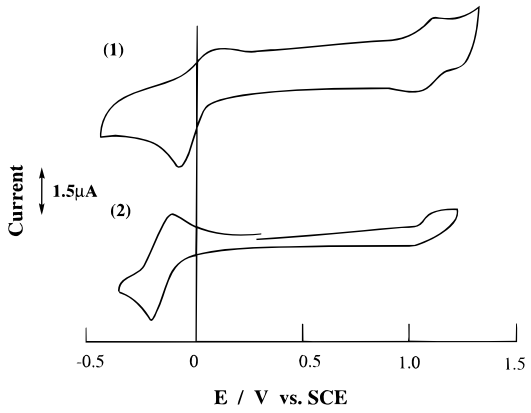

Figure 4. Cyclic voltammograms of **1** and **2** with glassy carbon electrode, platinum-plate electrode, and saturated calomel electrode as a working electrode, a counter electrode, and a reference electrode, respectively, with a scan rate of 1×10^2 mV s^{-1}, at a concentration of 1×10^{-3} M: (1) **1** in CH_3CN with 0.1 M tetra-*n*-butylammonium perchlorate (TBAP); (2) **2** in DMF with 0.1 M TBAP.

These results strongly indicate the presence of μ-oxo bridged high-spin ferric ions in **2**. Although **2** shows the largest ΔE_Q value, the Fe−O(μ-oxo) bond length of **2** (1.782 Å) is not so short compared with those of its related compounds (see Table 4). It seems, therefore, that ΔE_Q values do not correlate simply with the Fe−O(μ-oxo) bond lengths of the (μ-oxo)bis(μ-acetato)diiron(III) complexes.

The most important aspect is that the Mössbauer data for **2** are the closest to those for azido−metHr among the model compounds shown here. Considering the fact that the Mössbauer spectrum is very sensitive to subtle changes in coordination sphere, it may be concluded that L^2 in **2** provides a coordination environment very similar to the nitrogen donor sets in the active site of the azido−metHr.

The cryomagnetic properties of **2** are shown by the plot of χ_A vs T in the temperature range 80−300 K (Figure 3). The magnetic susceptibility per one Fe^{III} (χ_A) decreases with decreasing temperature. The result indicates a very strong antiferromagnetic spin-coupling between a pair of iron(III) ions. An excellent fit of the χ_A-T data to a dinuclear model is obtained when $J = -95$ cm^{-1}, g = 2.00, and paramagnetic impurity(%) = 0.007 are assumed for **2**. The J value of **2** is smaller than that of azido−metHr, but falls in the range of those values (−91 to −132 cm^{-1}) reported for the (μ-oxo)bis(μ-carboxylato)diiron(III) complexes.[2]

The cyclic voltammograms of **1** and **2** are shown in Figure 4, which exhibits two quasi-reversible redox waves at −0.01 and +1.10 V (vs SCE) for **1** and at −0.17 and +1.08 V (vs SCE) for **2**. These results indicate that both L^1 and L^2 provide a similar electronic environment for the iron atoms of the complexes. The first redox waves of **1** and **2** are higher than that reported for **4** by 0.36 and 0.20 V, respectively.[10d] Probably the pyridine π-nitrogen donors of both L^1 and L^2 stabilize the reduced Fe_2(II,III) states of **1** and **2** more effectively than the aliphatic nitrogen donors of 1,4,7-trimethyl-1,4,7-triazacyclononane of **4**.

Conclusion

Sessler et al.[13] and Toftlund et al.[14] reported that the dinucleating hexadentate ligands L^4 and L^5 form tetranuclear

complexes (**5** and **6**) consisting of two (μ-oxo)bis(μ-acetato)-diiron(III) core units. They also pointed out the difficulty of the synthesis of a discrete (μ-oxo)bis(μ-acetato)diiron(III) complex with a dinucleating hexadentate ligand. In the present study, however, we have succeeded in the synthesis and show the crystal structure determination of a discrete (μ-oxo)bis(μ-acetato)diiron(III) complex with the dinucleating hexadentate ligand L^2. Therefore, it is clear that a dinucleating hexadentate ligand does not generally afford a tetranuclear iron complex and the degree of the nuclearity of the complexes depends on the design of the spacer groups and/or the tridentate sites of the ligands. The number of carbon atoms of the alkyl spacer linking the two tridentate sites is two for L^2 and four for L^4 and L^5. The length of the spacer group might affect the nulearity of the complex as suggested by Sessler et al.[13] Another important point in this study is that **2** is structurally and spectroscopically very similar to the diiron center of the azido−metHr. It is concluded that (1) a discrete (μ-oxo)bis(acetato)-diiron(III) complex can be synthesized even with a dinucleating hexadentate ligand if the ligand is well designed for the formation of the dinuclear complex and (2) it is possible to prepare viable hemerythrin models by using well-designed dinucleating ligands.

Supporting Information Available: An X-ray crystallographic file, in CIF format, for **2**·DMF·2-PrOH·H_2O is available. Ordering information is given on any current masthead page.

IC9600994